

SST-IDDES Analysis of Vane-Induced Unsteady Mixing in a 4×4 Rod Bundle with Split-Type Mixing Vanes

Chaehyeon Song, Minseop Song^{a*}

Department of Nuclear Engineering, Hanyang University, 222 Wangsimni Rd., Seoul, 04763, Republic of Korea

*Corresponding author: hysms@hanyang.ac.kr

* **Keyword** : Turbulent mixing, Spacergrid, Mixing vane, SST-IDDES

1. Introduction

Spacer grids in pressurized water reactor (PWR) fuel assemblies serve dual functions: mechanical support of fuel rods and enhancement of subchannel mixing through mixing vanes. The inclined vanes generate transverse flow components and shear layers downstream of the grid, thereby disrupting thermal boundary layers and promoting inter-subchannel momentum exchange. Owing to their influence on heat transfer performance and critical heat flux behavior, spacer-grid-induced mixing has been a subject of sustained investigation in nuclear thermal-hydraulics.

Experimental studies have provided benchmark data on pressure drop, mean velocity distributions, and global mixing factors in rod bundles equipped with spacer grids. Such measurements have contributed significantly to validation efforts and code development. However, detailed characterization of three-dimensional unsteady wake structures remains limited due to spatial and temporal resolution constraints inherent in experimental diagnostics, particularly in the near-wake region immediately downstream of mixing vanes.

Computational fluid dynamics (CFD) has therefore been extensively applied to analyze spacer-grid-induced flows. Reynolds-averaged Navier–Stokes (RANS) models, including SST $k-\omega$ and Reynolds stress formulations, have demonstrated reasonable agreement with experiments in terms of mean flow distributions and pressure losses. Nevertheless, because RANS equations are time-averaged, they do not resolve unsteady vortex structures or transient shear-layer dynamics generated by mixing vanes. Therefore, the physical mechanisms governing the spatial development of unsteady mixing remain only partially captured in RANS-based analyses.

Large Eddy Simulation (LES) has been employed to overcome these limitations by directly resolving large-scale turbulent structures responsible for momentum transport. Previous LES studies have successfully captured detailed wake interactions and cross-flow patterns downstream of spacer grids. However, for realistic Reynolds numbers and full-length rod-bundle domains, LES requires extremely fine meshes and high computational cost, which limits its applicability for systematic parametric investigations.

Hybrid RANS–LES approaches, such as Detached Eddy Simulation (DES) and its improved variants, provide a practical compromise between computational efficiency and scale resolution. In DES-type approaches,

the boundary layer is treated in RANS mode and LES is activated in the outer flow. However, the original DES may switch too early inside attached boundary layers on refined grids, causing grid-induced separation and an extended RANS–LES grey zone. SST-IDDES mitigates these issues by applying a shielding/delay mechanism that maintains RANS behavior in attached near-wall regions while enabling a more robust transition to scale-resolving mode in separated shear layers and wakes. This modeling framework is therefore suitable for resolving geometry-induced unsteady structures in complex configurations such as spacer grids with mixing vanes.

While many studies have analyzed the decay phenomena in the wake region, the spatial evolution of geometry-induced unsteady structures under controlled inlet conditions has remained a challenging task. In many simulations, synthetic inlet turbulence or prescribed turbulence intensities are imposed, causing the inlet-generated fluctuations to overlap with the geometry-induced fluctuations. Under such conditions, it is difficult to isolate the unique unsteady behavior generated solely by the spacer-grid geometry.

The present study investigates the spatial development and downstream attenuation of spacer-grid-induced unsteady mixing in a 4×4 rod bundle equipped with split-type mixing vanes using the SST-based Improved Delayed Detached Eddy Simulation (SST-IDDES) model. A uniform inlet velocity condition is prescribed without synthetic turbulence forcing to minimize externally imposed fluctuations and to emphasize wake structures generated by shear-layer instability and flow separation induced by the mixing vanes. The downstream evolution is analyzed on multiple cross-sectional planes downstream of the vane tips using instantaneous velocity-magnitude contours and in-plane velocity vector fields, and the attenuation of mixing intensity is quantified using plane-averaged transverse RMS velocity fluctuations and a reference in-plane velocity.

2. Methodologies

2.1 Analysis domain and boundary conditions

A 4×4 rod bundle equipped with a spacer grid incorporating split-type mixing vanes is selected as the analysis target. The spacer grid consists of symmetrically arranged split-type vanes at each intersection, and each vane is inclined at 30° relative to the main flow direction

(z-direction), thereby inducing cross-flow and promoting inter-rod mixing.

The rod diameter (D) and pitch are set to 30 mm and 40.95 mm, respectively, yielding a pitch-to-diameter ratio of $P/D = 40.95/30 \approx 1.37$. In the present work, axial locations are reported in a rod-diameter-normalized form as z/D .

The detailed geometry of the spacer grid, including grid straps, dimples, and mixing vanes, is shown in Fig. 1. A 4×4 configuration provides a representative internal subchannel arrangement and captures key mixing-vane interactions while maintaining computational feasibility for scale-resolving simulations over multiple downstream locations. Accordingly, the present domain is adopted to investigate spacer-grid-induced mixing mechanisms and unsteady wake development rather than full-scale assembly performance predictions.

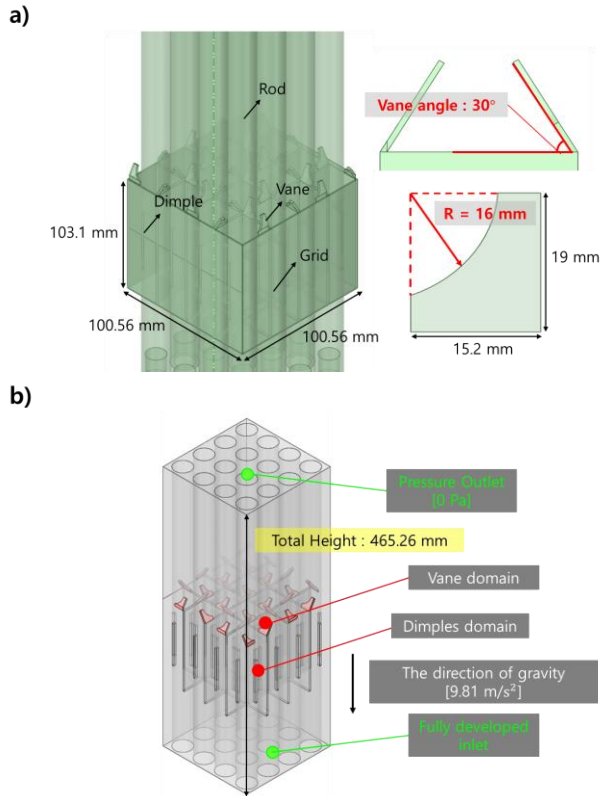


Fig. 1. Split-type mixing-vane spacer grid and computational domain. (a) Spacer-grid geometry (vane inclination 30°). (b) 4×4 rod-bundle flow domain and boundary-condition locations.

The simulations are performed on the fluid domain only. The rods and spacer grid are treated as no-slip walls, and the computational domain is defined as the flow volume obtained by subtracting the solid geometries. The total axial length of the main spacer-grid domain is 465.26 mm, consisting of an upstream section, the spacer-grid (vane) section, and a downstream section to capture wake development.

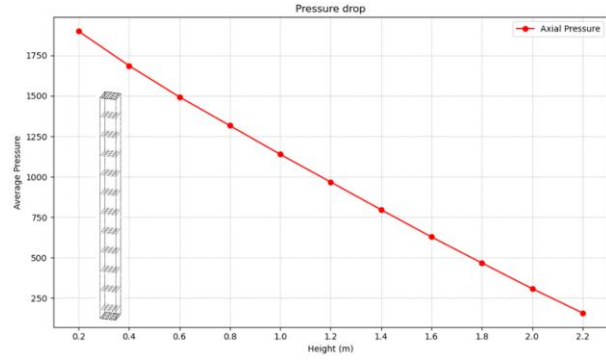


Fig. 2. Axial variation of cross-section-averaged static pressure in the auxiliary 90D domain, demonstrating fully developed flow.

To supply a fully developed inflow condition to the main spacer-grid domain, an auxiliary straight-pipe domain with an axial length of $90D$ is computed separately. A uniform bulk velocity of 1.5 m/s is prescribed at the inlet of the auxiliary domain, and the resulting fully developed outlet profile is mapped onto the inlet plane of the main spacer-grid domain. Accordingly, the inlet condition of the main domain is not a uniform velocity boundary; it is a mapped, fully developed profile obtained from the auxiliary computation.

The mapping procedure transfers not only the mean velocity profile but also the turbulence quantities required by the SST-IDDES formulation (e.g., k and ω) from the auxiliary-domain outlet to the main-domain inlet. No additional synthetic turbulence forcing is applied at the inlet; the resolved unsteadiness in the downstream wake is generated by geometry-induced separation and shear-layer instabilities downstream of the mixing vanes. At the outlet, a zero-gauge static pressure condition is applied ($P_{out} = 0$ Pa). Gravitational acceleration is included in the axial (z) direction, yielding an approximately linear axial variation of the cross-section-averaged static pressure as shown in Fig. 2. The Reynolds number, based on the rod diameter D , is approximately 44,910 under the present conditions ($\rho = 998.2$ kg/m³, $\mu = 0.001$ Pa·s). The computational domain and boundary conditions are summarized in Fig. 1.

2.2 Parametric study set-up and solver setting

In hybrid RANS–LES simulations, grid adequacy is commonly evaluated based on the capability to resolve separated shear layers and wake unsteadiness, rather than solely on residual convergence. Spacer-grid flows involve concurrent shear-layer formation, separation, and reattachment, and insufficient resolution in these regions may compromise the fidelity of the resolved unsteady structures. Accordingly, the mesh design follows the Young–Person’s Guide to Detached-Eddy Simulation (DES) grids, emphasizing adequate near-wall resolution with prism layers, sufficient refinement in separated and wake regions to enable scale-resolving behavior, and controlled RANS–LES transition to mitigate grey-zone effects and grid-induced separation.

Polyhedral cells are employed in the core region to enhance robustness for the complex spacer-grid geometry. A mesh-sensitivity study is conducted using multiple grid levels, and representative mesh distributions near the rod/wall and mixing-vane regions are shown in Fig. 3.

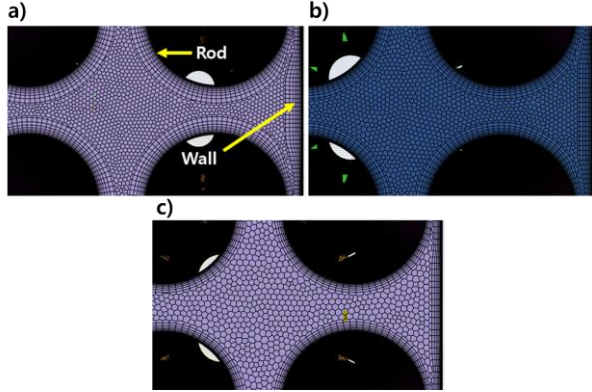


Fig 3. Mesh topology and local refinement near solid boundaries and mixing vanes. For each view: (a) fine, (b) medium, and (c) coarse grids

Mesh-sensitivity tests were conducted with the SST-IDDES model on the candidate grids to select a reference mesh. Grid adequacy was evaluated by comparing velocity profiles at selected axial locations and the overall pressure drop between the inlet and outlet. Refinement from the coarse to the medium grid significantly reduced the differences in both quantities, whereas further refinement to the fine grid produced only marginal changes in the monitored quantities. Accordingly, the medium grid was selected as the reference mesh for the SST-IDDES simulations as a practical compromise between spatial resolution and computational cost.

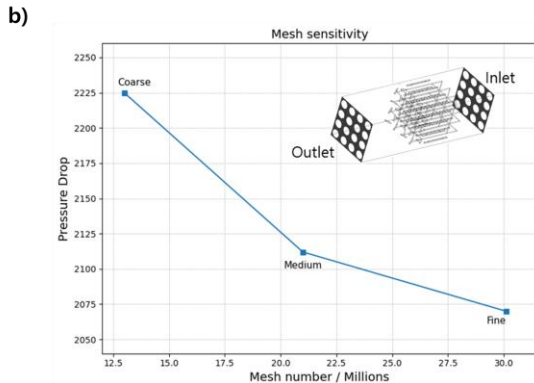
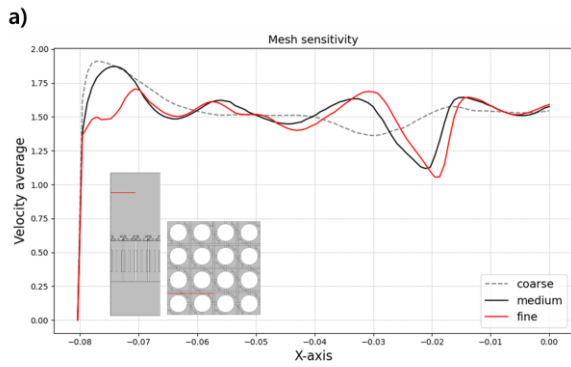


Fig 4. Mesh-sensitivity assessment: (a) Velocity profiles along the transverse line and (b) Global pressure drop across the domain for coarse, medium, and fine meshes.

The characteristics of the selected reference (medium) grid are summarized in Table 1.

Table 1. Mesh characteristics for the medium used in the SST-IDDES simulations.

LES region mesh size	0.7 mm
RANS region prism layers	13 layers
Growth rate	1.32
First layer thickness	0.03 mm
Last layer thickness	0.7 mm
y^+	1.047
Total prism thickness	2.477 mm
Total Cells [Millions]	15.7

In the present study, unsteady wake structures downstream of the mixing vanes are simulated using the SST-IDDES framework. To isolate geometry-driven fluctuations, a uniform inlet condition is imposed without synthetic turbulence forcing, so that the resolved unsteadiness originates primarily from vane-induced separation and shear-layer instability rather than from inlet-generated disturbances. This approach enables a tractable yet scale-resolving prediction of spacer-grid wakes in the 4×4 rod-bundle configuration and supports the plane-based statistical analyses used to quantify downstream attenuation of mixing intensity.

Table 2. Solver settings and numerical parameters for IDDES simulations.

Setting	DES
CFD Tool	Ansys FLUENT
Turbulence model	SST-IDDES
Solver	Pressure based
Wall condition	No-slip condition
Fluid material	Water (Density : 998.2 [kg/m ³], Viscosity : 0.001 [Pa·s])
# of time step	4000
Timestep size	0.001 s
Courant number	0.5
Subgrid model	WALE

3. Results

3.1 CFD analysis results

This section presents the downstream evolution of spacer-grid-induced mixing based on the SST-IDDES simulations. The quantitative discussion focuses on unsteady flow features resolved by SST-IDDES and plane-based spatial statistics, aiming to characterize how cross-flow intensity and transverse velocity fluctuations

evolve with axial distance downstream of the mixing vanes.

A plane-based post-processing strategy is adopted to examine the spatial development of the spacer-grid wake. Multiple axial planes ($z1-z6$) are defined downstream of the spacer grid with the origin ($z=0$) set at the vane-tip location. The axial locations of the evaluation planes are defined in terms of the dimensionless distance z/D , allowing systematic characterization of both the near-wake ($z/D \lesssim 2-3$) and the developing wake regions. On these planes, instantaneous velocity magnitude and in-plane velocity vectors are analyzed to interpret the spatial evolution of vane-induced mixing structures.

For consistent downstream comparison using representative plane-averaged statistics, three reference planes corresponding to $z/D = 2, 4$, and 6 are additionally selected, on which plane-averaged transverse RMS and the reference in-plane velocity are evaluated. All plane-averaged quantities are computed using an area-average operation over the evaluation-plane surface. All analysis planes are cross-sectional $x-y$ planes normal to the main flow direction (z -direction); therefore, the in-plane velocity components correspond to the transverse velocity components $u(x,y,t)$ and $v(x,y,t)$ on each evaluation plane.

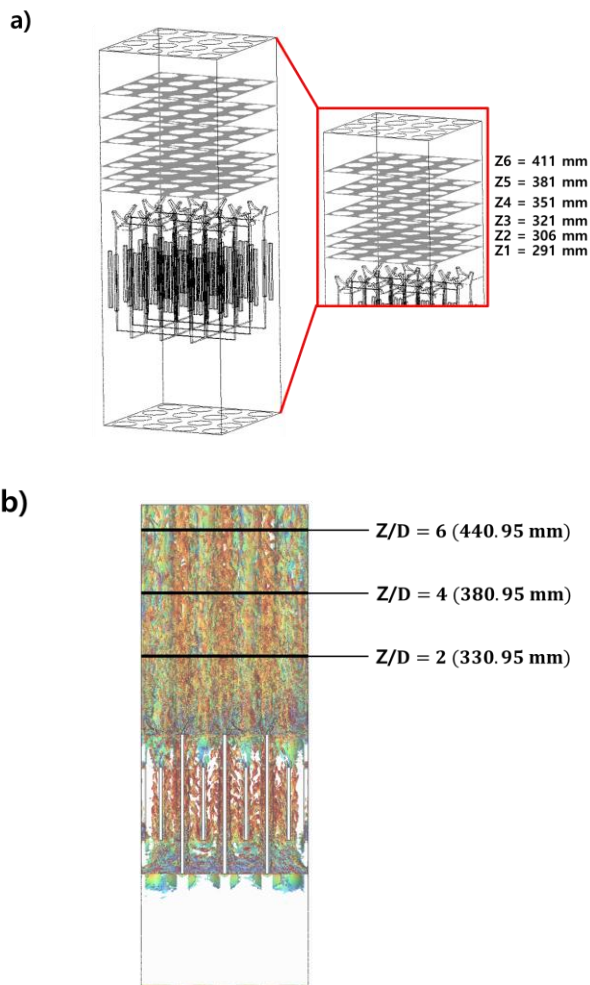


Fig. 5. Locations of the analysis planes used for plane-based evaluations downstream of the spacer grid.

The instantaneous velocity magnitude fields (Fig. 6) show that, in the near-wake region immediately downstream of the vane tips ($z1-z2$), locally accelerated jet-like features form in the vicinity of the vane-tip region. Further downstream ($z3-z4$), the high-velocity region spreads laterally while the local peak becomes less pronounced, suggesting that the momentum initially concentrated near the vane tips is redistributed across the subchannel cross-section through lateral transport and mixing. In the far-wake planes ($z5-z6$), the cross-sectional velocity field appears more uniform with reduced extreme high- and low-velocity patches, indicating progressive attenuation of the vane-induced non-uniformity. The gradual dissipation of mixing energy as the flow evolves downstream.

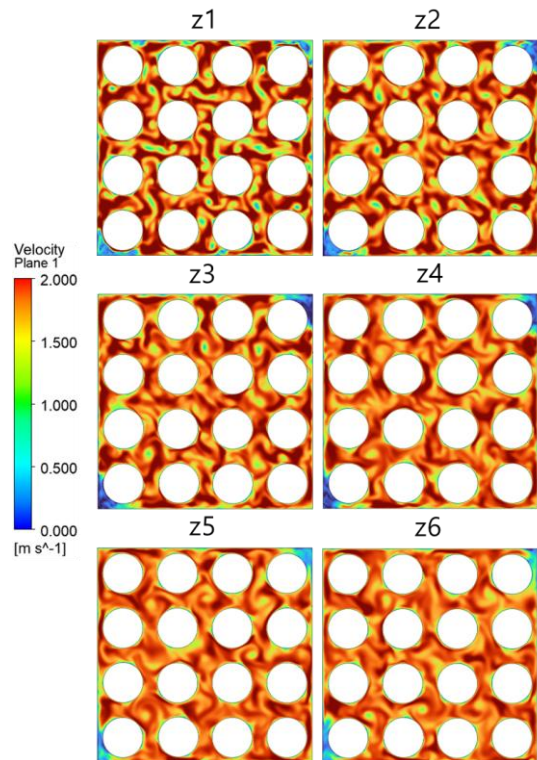


Fig. 6. Instantaneous velocity-magnitude contours on planes $z1-z6$ downstream of the vane tips (snapshots).

The in-plane velocity vector fields (Fig. 7) reveal cross-flow structures associated with lateral mixing. In the near-wake planes ($z1-z2$), pronounced transverse velocity components are observed across rod gaps in addition to the axial flow, indicating cross-flow generation by the inclined vanes. With increasing axial distance ($z3-z4$), the transverse components weaken and the vectors become more aligned with the main flow direction, suggesting attenuation and partial merging of the vane-induced lateral structures. In the far-wake region ($z5-z6$), the cross-flow patterns appear more diffuse and fragmented, indicating reduced spatial coherence of the vane-driven lateral motion.

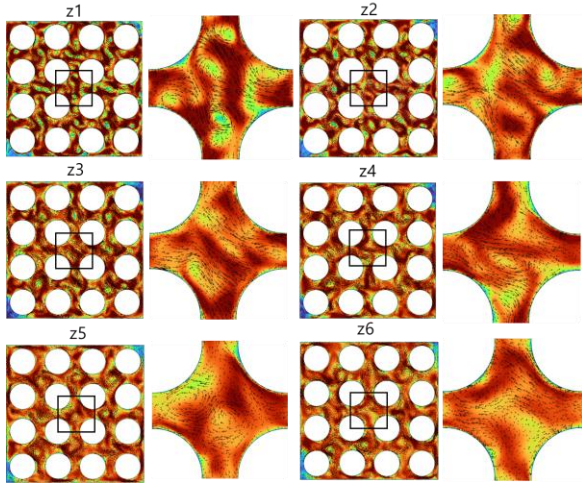


Fig. 7. Instantaneous velocity vectors on planes z1–z6 showing spacer-grid-induced cross-flow structures (snapshots).

The downstream attenuation of lateral mixing intensity is quantified using plane-averaged metrics on the reference planes at $z/D = 2, 4,$ and 6 . The plane-averaged transverse RMS velocity fluctuation is defined as:

$$\text{RMS}_{\text{transverse, plane}} = \sqrt{\frac{1}{A} \int_A \langle u'(x, y, t)^2 + v'(x, y, t)^2 \rangle_t dA}$$

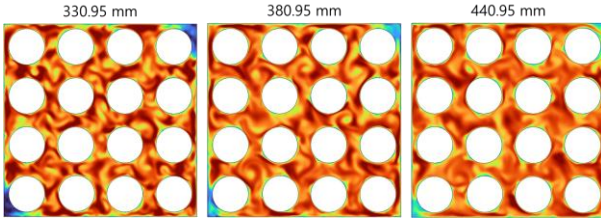


Fig. 8. Instantaneous in-plane velocity magnitude at $z/D = 2, 4,$ and $6,$ with $\text{RMS}_{\text{transverse, plane}}$ indicating downstream decay of lateral mixing.

Instantaneous fields are presented as snapshots at a representative time, whereas statistical quantities are evaluated after excluding the initial transient. The simulation is run for 4 s with a fixed time step of $dt = 0.001$ s, and statistics are computed over the statistically stationary interval $t = 1-4$ s. The fluctuating components are defined by subtracting the local time-mean at each (x, y) :

$$\begin{aligned} u'(x, y, t) &= u(x, y, t) - \langle u(x, y, t) \rangle_t \\ v'(x, y, t) &= v(x, y, t) - \langle v(x, y, t) \rangle_t \end{aligned}$$

where $\langle \rangle_t$ denotes time averaging over $t = 1-4$ s. $\text{RMS}_{\text{transverse, plane}}$ represents the area-averaged magnitude of in-plane velocity fluctuations and is used as a measure of vane-induced lateral mixing. Over the present reference planes, $\text{RMS}_{\text{transverse, plane}}$ shows a

decreasing trend from 0.2196 m/s at $z/D = 2$ to 0.2136 m/s at $z/D = 4$ and 0.2053 m/s at $z/D = 6$, indicating downstream attenuation of transverse velocity fluctuations under the present condition. In addition, the plane-averaged mean in-plane velocity magnitude is computed as the time- and plane-averaged in-plane speed magnitude:

$$U_{\text{transverse}} = \frac{1}{T} \int_{t_0}^{t_0+T} [\langle \sqrt{u(x, y, t)^2 + v(x, y, t)^2} \rangle_A] dt$$

where u and v are the in-plane velocity components on the evaluation plane and $\langle \rangle_t$ denotes time averaging over the statistically stationary interval. Over the present reference planes, $U_{\text{transverse, plane}}$ decreases from 0.3303 m/s at $z/D = 2$ to 0.2798 m/s at $z/D = 4$ and 0.2428 m/s at $z/D = 6$, indicating downstream attenuation of the overall in-plane motion level. The decreasing trends of both $\text{RMS}_{\text{transverse, plane}}$ and $U_{\text{transverse}}$ are consistent with the qualitative observations from the instantaneous velocity magnitude and vector fields, supporting that spacer-grid-induced mixing is strongest in the near-wake region and weakens further downstream under the present condition.

Overall, the SST-IDDES results suggest that (i) locally high-speed, jet-like features and strong shear layers form immediately downstream of the mixing vanes, (ii) distinct cross-flow patterns are most pronounced in the near-wake region and weaken with increasing axial distance, and (iii) the plane-averaged mixing metrics show a decreasing trend over the present reference planes, supporting quantitative assessment of the downstream attenuation of spacer-grid-induced mixing.

4. Conclusions

This study demonstrates that spacer-grid-induced mixing evolves downstream through a consistent sequence of shear-driven generation, spatial redistribution, and gradual attenuation. Using SST-IDDES under a uniform inlet condition, geometry-induced unsteady mixing structures generated intrinsically by the spacer grid are examined through plane-based analyses.

The results show that strong shear layers and transverse flows are generated near the mixing vanes, producing intense lateral motions in the near-wake region. Consistently, plane-averaged measures of lateral mixing intensity—represented by the transverse RMS velocity fluctuation and the reference in-plane velocity—decrease monotonically with axial distance, confirming progressive attenuation of vane-induced cross-flow and mixing.

These unsteady wake features and their downstream evolution are not adequately represented by time-averaged approaches, whereas SST-IDDES resolves the relevant unsteady structures while maintaining stable near-wall behavior, making it suitable for analyzing spacer-grid wake dynamics.

The present study focuses on analyzing the attenuation of vane-induced flow rather than providing a predictive assessment of absolute mixing performance. Future work will focus on experimental validation using the same spacer-grid geometry.

ACKNOWLEDGMENT

This research was supported by the National Research Council of Science & Technology (NST) grant by the Korea government (MSIT) (No. GTL24031-000). This work was supported by the Korea Institute of Energy Technology Evaluation and Planning (KETEP) and the Ministry of Climate, Energy and Environment (MCEE) of the Republic of Korea (No. RS-2024-00398867).

REFERENCES

- [1] M. S. Gritskevich, A. V. Garbaruk, J. Schütze, and F. R. Menter, "Development of DDES and IDDES formulations for the $k-\omega$ shear stress transport model," *Flow, Turbulence and Combustion*, 88, 431–449 (2012).
- [2] E. E. Dominguez-Ontiveros, Y. A. Hassan, M. E. Conner, and Z. Karoutas, "Experimental benchmark data for PWR rod bundle with spacer-grids," *CFD4NRS-3 Technical Papers*, OECD/NEA/CSNI (2012).
- [3] P. R. Spalart, *Young-Person's Guide to Detached-Eddy Simulation Grids*, NASA/CR-2001-211032, NASA Langley Research Center (2001).
- [4] J. Xiong, W. Qu, T. Zhang, X. Chai, X. Liu, and Y. Yang, "Experimental investigation on split-mixing-vane forced mixing in pressurized water reactor fuel assembly," *Annals of Nuclear Energy*, 143, 107450 (2020).
- [5] F. Wiltschko, W. Qu, and J. Xiong, "Validation of RANS models and Large Eddy simulation for predicting crossflow induced by mixing vanes in rod bundle," *Nuclear Engineering and Technology*, 53, 11, 3625–3634 (2021).